Energy Management for a Random Outage Grid-tied Hybrid Photo-voltaic Solar-Thermal Energy System for health Center Applications

Z. S. Johnson[1*], C. N. Nimyel[2], K. P. Muar[3] and D. P. Cornelius[4]

1. Department of Mechanical Engineering, Plateau State Polytechnic Barkin Ladi, Nigeria.
2. Department of Computer Engineering Plateau state, Nigeria.
3. Department of Mechanical Engineering, University of Jos, Nigeria.
4. entre for Signal and Image Processing, University of Strathclyde, Glasgow, United Kingdom.

Abstract

This research work proposes and evaluates an enhanced open-loop photo-voltaic evacuated tube solar thermal collector hybrid energy system based on the developed multi-objective energy management strategy that manages and coordinates the hybrid system with a randomly unreliable grid power source to meet the health center's energy demand using the TRNSYS software. A technical assessment of the system shows that the system is capable of meeting system load with a solar fraction of 67% even on days with an overcast sky level of radiation as low as 250 W/m^2 and only 37.5% grid power availability. Overall, the system has a solar fraction of 80%. The implication of an 80% solar fraction is the large environmental benefit of reducing emissions and improved system economic viability, indicating that the formulated energy management achieves the goal of promoting renewable energy sources in the hybrid system. An economic analysis of the system revealed that it has a payback period of 6.9 years and net present value of $36,985 at the end of the project's lifetime. This demonstrates that the upgrade of the traditional hybrid PVT with an evacuated tube collector operated based on the developed energy management strategy has met the goal of minimizing emissions with significant environmental and economic savings.

Keywords: *Multi-objective energy management, Hybrid PVT collector, Payback period, Net present value, Grid connected.*

1. Introduction

Most developing countries' power is grossly inadequate, going by their population [1]. Moreover, frequent and unpredictable outages are the dominant characteristic of grid power in most developing countries, as reported by the recent report released by the International Finance and Cooperation (IFC) in the meantime, the hybrid energy system, which combines conventional and renewable energy systems, is unarguably the option that offers the best compromise between the economic and environmental protection for communities with low access to grid power [2]. For example, the photovoltaic-solar thermal energy system is a technology that simultaneously produces both power and thermal energy suitable for application in the building sector since its energy demand is predominantly power and thermal energy. Even though the great potential of the hybrid PVT energy system is a good match for residential applications, its wide adoption in many locations is still a challenge [3]. The low installed capacity of renewable power despite reported good potential [4]–[6] and persistent energy crisis is evidence of these obstacles.

Amirmohammad *et al.* [7] provided a novel, practical, and cost-effective solution to reduce the environmental impact of smart building energy systems and promote greater use of renewable energy in the construction industry. This solution is based on the use of a rule-based automation approach that takes into account thermal comfort, energy prices, meteorological data, and primary energy use.

For successful hybridization of renewable energy resources with a randomly unreliable grid power, selecting an energy management strategy that ensures optimal and dependable operation is necessary to deliver on the desired objective. Understanding the most important performance criteria such as system reliability, solar fraction, and profitability indices of return on investment and net present worth among others depending on

the desired objective, is the only way to arrive at the best technical and financial solution [8]. For example, the ideal technological consideration for a hybrid system with battery storage is to keep the battery's operational status at 20% to 30% depth of discharge (DOD), and replaces the battery when its capacity falls to 80% of its nameplate capacity[9]. The control approach adopted by [10] is designed to lower the system operating costs of a hybrid energy system comprising of a solar panel, wind turbine, and fuel cell connected to grid power.. Similarly, in one study, to ensure that load demand is met satisfactorily with optimal economic value, a Genetic Algorithm (GA) is used for the coordination and operation of a hybrid PV/FC/battery system [11]. An energy management strategy (EMS) whose goal is to minimize the total life cycle cost while ensuring demand is met was proposed by [12]. The concept of load shifting was employed by [13] to coordinate the utilization of energy storage from a hybrid photovoltaic and wind with battery storage integrated with a grid power system. The result shows that the ideal load shifting in the control strategy resulted in a 25.66 % decrease in energy cost and a 91.72 % decrease in battery degradation cost compared to the simple basic control without load shifting when discharging the battery [13].

In an attempt to increase distributed energy system stability and reliability, a new control mechanism incorporating day-head demand response energy for the management of rural standalone energy systems was formulated [14]. Based on the objective of balancing power supply with the load demand [15] proposed based on a rule-based energy management algorithm, a smart energy management system for a grid coupled hybrid solar/wind/biomass. A flexible multi-winding magnetic link operating in both grid-connected and off-grid modes is proposed to synchronize the energy operation from PV panels and fuel cells with battery bank storage. The goal was to have a real-time rule-based controller that controls the power flow in the system optimally based on the desired objective. The analysis of the results revealed a reduction in total energy costs for grid utilization from 2.13 $/day to 0.315 $/day [16]. The sizing methodology of a hybrid renewable energy system that utilizes the economic predictive model energy management approach was investigated for a standalone hybrid wind/PV system with hydrogen and battery storage [17]. In another study, a cost-effective algorithm for optimizing the operation of a hybrid renewable smart grid distribution system was

proposed. The proposed algorithm is focused on maximizing the use of renewable energy sources while simultaneously minimizing the overall cost of meeting the load demand. Furthermore, the batteries are also controlled by an intelligent energy technique that forecasts and discharges the battery only when there is no significant load expected in the near future [18]. An evaluation of a hybrid energy system consisting of photovoltaic panels, hydrokinetic, wind turbine, battery storage, and diesel generator for power generation under Persian Gulf Islands weather conditions was carried out by [19]. An investigation by [20] revealed that the adoptive model control strategy used to control the ground source heat pump (GSHP)-PVT hybrid system increased electricity production by 4.4% and 6.2% during cooling and heating, respectively. Sanjel and Baral [152] compare the grid power option with a photovoltaic hybrid energy system with diesel and battery storage as backup for power supply in rural communities of Nepal. The authors concluded that the grid power source is favorable with reduced cost of fossil-based power generation, whereas for islanded communities with low power demand, photo-voltaic energy systems with battery and diesel generator provides reliable and affordable power alternative. Similarly, energy management for a micro-grid system with a wind/PV/Battery system based on battery state of charge (SOC) was designed and assessed by Liu *et al*. [21]. The authors concluded that an intelligent decentralized energy system with wind /PV/battery meets the designed load with good reliability and provides a quick, smooth, and steady state of the switchover of the system.

According to [125], an adoptive model control method employed to control the GSHP-PVT hybrid system resulted in a 4.4% and 6.2% increase in power generation. [22] investigated a grid-connected hybrid renewable energy system controlled based on the improved particle swarm optimization technique. Allouhi *et al*. [23] assessed the energetic performance of a grid integrated hybrid PVT energy system for building application using the TRNSYS software employing an energy management strategy that control a hybrid energy system that consist of PVT/Wind/storage tank integrated with reliable grid power. The control strategy was based on a simple load balance ensuring system reliability. The economic performance indicator revealed a solar fraction of 64.8%, a self-sufficient ratio (SSR) of 90.25% and a self-consumption ratio (SCR) of 43.08%. The lower SCR means about

57% of the power produced by the renewable energy system is sold back to the grid. However, whether the system has a positive Net Present Value (NPV) is unclear. Behzadi *et al*. [7] used a supply-demand side energy management technique to coordinate a hybrid PVT and biomass energy system integrated with the national grid to fulfil building thermal and power demand in Stockholm. The proposed system is based on a rule-based automation method that takes into account the study location's thermal comfort, energy pricing, meteorological data, and primary energy use. The goal is to reduce energy costs and carbon emissions by minimizing the footprint of smart building energy use. As a result, 61% of the renewable energy generated was utilised to meet demand in the facility, suggesting a significant economic savings. The system has the ability to reduce CO_2 emissions by 70 tons per year.

A wide range of literature has reported studies on hybrid PVT energy systems integrated with reliable or grid with scheduled outages for domestic application. However, in developing countries grid power is highly characterized by frequent outages [24], [25]. Critical sectors like the health facilities cannot deliver quality health services without adequate and reliable power. There is the need to find alternative power to grid power to support critical sectors like health centers.

According to the review, no study has been examined for hybrid PVT integrated to a randomly unavailable grid power source based on an open loop cooling control method for use in critical sectors such as hospitals. This study develops and tests a novel open-loop photovoltaic evacuated tube solar thermal collector hybrid energy system (OPVETC) connected to a grid with random power loss. The goal is to develop an energy management system that manages and coordinates the OPVETC hybrid PVT with a randomly unreliable grid power source in order to meet the health center's power and hot water demand in a more efficient and cost-effective manner, resulting in a significant increase in the system's economic net worth and environmental protection.

For this study, the random power failure grid connected OPVETC is used to meet the power and hot water demand of a typical health center located in Jos to demonstrate the benefit of the system and energy management strategy. Consequently, the OPVETC is modelled using the TRNSYS 18 software, and simulated and assessed based on the developed multi-objective Energy Management strategy (EMS) that meets total building power and hot water demand in the most reliably, economical, and environmentally friendly manner. An economic and environmental assessment of the proposed system based on the simulated performance using TRNSYS software under weather data of Jos, Nigeria was conducted to evaluate the benefits of the new system operated based on the developed energy management system.

2. Materials and method
In this section, a simple description of the open-loop photovoltaic evacuated tube solar thermal collector hybrid energy system (OPVETC) coupled to a grid characterized by random power failure is presented. The approach for the modeling of the system is also presented. Furthermore, the system's energy management and operating strategy for the control and coordination of the OPVETC is also formulated.

### 2.1. Description of study location and energy system
The proposed OPVETC hybrid energy system consists of the evacuated tube collector (ETC) and the sheet-and-tube PVT collector array. Two hot water storage tanks are included as additional components. To store extra power produced by the PV panel, a battery storage system is included. As a backup, a small diesel generator set is added in case the building's demand cannot be met by renewable energy. A smart microcontroller integrates the hybrid energy system, the small diesel generator, and the inconsistent grid power sources to efficiently coordinate the power produced by the power element to efficiently fulfil the energy demand of a health center. The full methodology starts with the modelling of the energy systems, comprising of the unreliable grid power, the diesel generator, and OPVETC. After the energy systems modelling, the building load is estimated and finally the energy management and flow control strategy that coordinates the system is further developed, as illustrated in figure 1.

2.2. Energy system modelling approach
In this study, the transient system simulation tool TRNSYS 18 is selected for the system modelling, performance simulation, and evaluation. TRNSYS 18 is a modular software package with a comprehensive library of validated components like the PVT collector [187] [188] models that can be customized to any conceived energy solution and with great flexibility for adaptation for different applications.

A detail dynamic model as seen in **Figure 2** of the system, as depicted in the schematic as shown in **Figure 1**, is developed as a representation of the actual system to predict the system performance and evaluate the annual performance under the actual load and weather conditions of the case study using the TRNSYS 18 software. This model consists of the various system components referred to as 'Type' found in the simulation library. The model components are connected in a manner that represents the actual working of the real system. The function of each component of the model is explained in table 1 below.
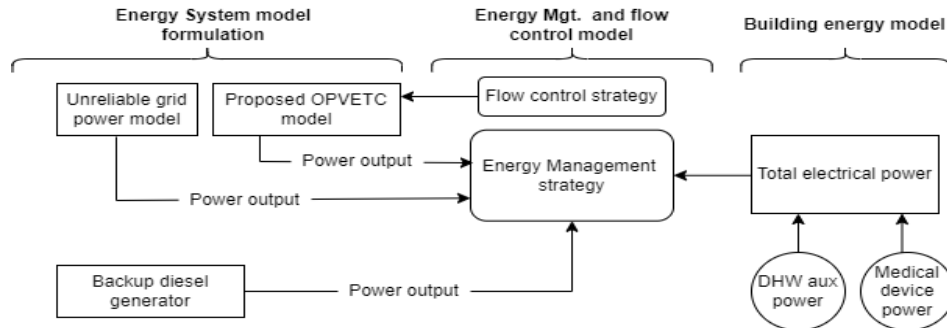
Figure 1. Schematic representation of the energy system and energy management technique.
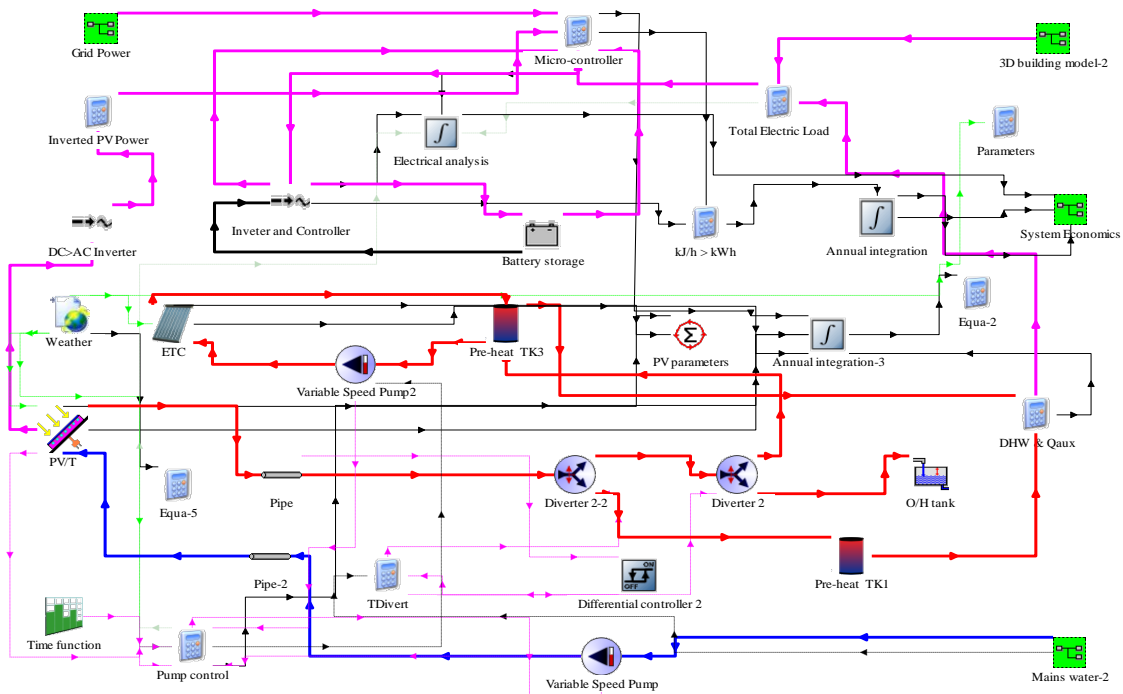
Figure 2. Detail dynamic TRNSYS model of the OPVETC hybrid energy system.

Table 1. OPVETC system components model and their functions.

Name	Type	Function/Action
Weather processor	Type 15	It serves to process the weather data from an external weather data file at a given time step and make it accessible to other components of TRNSYS.
PVT collector	Type 560	The type 560 models an un-glazed sheet and tube PVT collector that produces both powers from the PV module and hot water from a fluid stream passing under the PV module used to cool it.
Evacuated tube collector	Type 71	This component models the thermal performance of a variety of an evacuated tube collector.
Solar pump	Type 110	Models a variable speed solar pump that circulates the cooling water through the solar collectors. Controlled by input from other controllers.
Forcing function	Type 14	Models the hot water demand load profile. The output of this component serves the purpose of presenting the hot water drawn from the tank.
Diverter	Type 11	This component splits a fluid stream into two streams according to the user-specified ratio.
Battery storage	Type 47	Models a lead-acid battery storage system. The model accepts power as input to charge the battery and outputs power to meet the load.
Inverter/ regulator	Type 48	The function of this component is to convert the direct current (DC) to alternating current (AC).
Hot water storage tank	**Type 158**	**This unit models the thermal behavior of a vertical hot water storage tank with two inlets and outlets. Interacting with the hot fluid inside the tank and environment to predict the temperature of the fluid content.**
Equation blocks	-	The equation blocks are not found in the library as the rest of the components. They are used to develop energy and flow control strategies that control the system to effectively meet energy demand. It is equally valuable for evaluating the performance of the system

2.3. Energy management and dispatch strategy

For this study, the proposed energy management and the grid dispatch strategy is based on the Follow-Electric-Load (FEL) control strategy that prioritizes power from the PV module to meet the load. For this strategy, the various power elements in the system are set to produce the electric and thermal energy that follows the thermal power demand pattern and extra steps to ensure that excess of what is required is minimized. The PVT power production is first used to meet power demand, and the excess is used to charge the battery. Power from the grid is only taken when power from the PVT collector is insufficient to meet the load completely, and the battery power has been discharged to 20% of its storage capacity. In other words, when the PVT power is not adequate to meet power demand, the battery storage power is called to be used first and must be expended to 20% of the battery storage capacity before the grid power can be dispatched if available. In this study, the battery's maximum, and minimum state of charge (SOC) limits are set at 80% and 20%, respectively, in order to ensure its security to extend the battery life [28], [29]. Notably, for periods where the PV power is unavailable, the grid power is used to meet load and equally charge the battery until the battery is fully charged or the grid goes off due to outage. Consequently, when the PV power is unavailable, the grid power dispatched is modelled as power sufficient to meet load demand and charge the battery until the battery state of charge (BSOC) is

100% as illustrated in flow chart in figure 4. In this study, the excess power generated is dumped when the load is fully met and the battery state of charge is 100%, as this is the right scenario in most developing countries with unstable grid power [24], [25] and with no feedback tariff grid policy. The flow chart and the control logic for the energy management control and dispatch strategy are shown in figure 3 and figure 4.

Since grid energy is dispatchable when available, and the grid power source in this study is characterized by random failure, a model has also been developed that predicts the grid power dispatched. The developed model predicts the grid availability and unavailability and decides how much grid power is required at each step to avoid taking excess grid. Figure 4 is a flow chart of how the grid operation was modelled. Under this control operation, the grid power charges the battery only when there is no excess power from the PV or the excess power is not sufficient to charge the battery to 100% of its capacity. In other words, for the period where the PV power is entirely unavailable, the grid power is modelled as the total electric power demand of all the building appliances plus the battery maximum charging power for a battery with a state of charge (BSOC) less than 100%. When the PV power is available, grid power can only be dispatched as the balance required to meet the unmet load by PV and the maximum charging power needed to charge the battery to 100% of its power capacity as illustrated in the flow chart in figure 4.

Figure 3. Detailed control logic and the modelled energy management strategy.
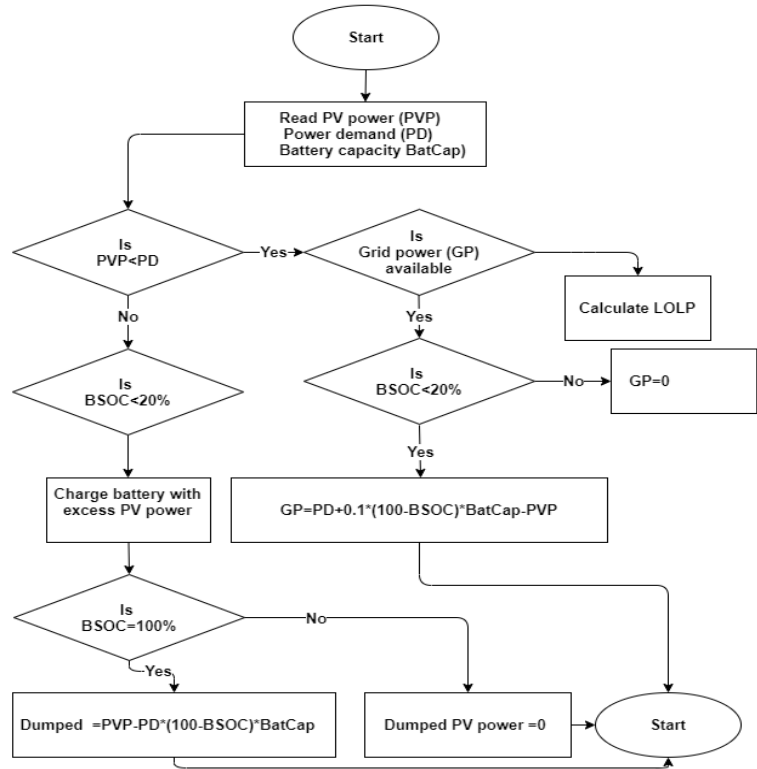
Figure 4. Flow chart model of grid power dispatch.

2.4. Validation and verification of system model

It is a common practice to determine whether a formulated system model and its outputs are valid, and to a large extent, represent the actual system and its outputs. In this study, the verification and validation (V & V) methodology as used by Sigarchian [30] to validate a small-scale polygeneration energy system, is adopted. By this technique, the closeness of the conceptual model to the actual system and its outputs are ascertained. The V & V verification approach compares component-by-component outputs of the formulated components of the modelled system to the description of the expected theoretical behavior as found in the literature. To this end, different studies have experimentally validated the Type 560 of the PVT collector model found in the simulation library of TRNSYS [26], [27], [31]–[33]. Similarly, Type 56 of the 3D building model found in TRNSYS have been experimentally validated in other studies[34], [35]. Furthermore, the simulated output of the evacuated model (Type 73) was found to be 13.7% variance with the experimental result under a quasi-steady state in a study conducted by [36]. In addition, an energy balance analysis to check the relative accuracy of the formulated system

model was conducted utilizing an energy balance subroutine (Type 28) obtained in the TRNSYS library. This subroutine (Type 28) checks and compares the energy flows across the system boundary and determines if the flow across the system boundary is balanced. Energy flows (losses and gains) of several components of the entire system are linked to this component specifying whether it's a loss or a gain. For this method, the system power and thermal boundaries of system components are analyzed separately, as shown in figure 5. The yellow arrow shows all gains across a component boundary with direction pointing into the boundary. Likewise, all losses are indicated by the arrow pointing outwards of the boundary. All losses have a negative convention for analysis, and all gains are assigned positive values. The simulation summary subroutine (Type 28) performs the monthly and annual arithmetic on all energy quantities connected to it. Consequently, if the energy balance between the system gains and losses is within a 2% error, then the formulated model is appropriately set up, and the simulated model converges within the specified time step and tolerance error; otherwise, a warning will be issued in the *.lst and *.log file [37].
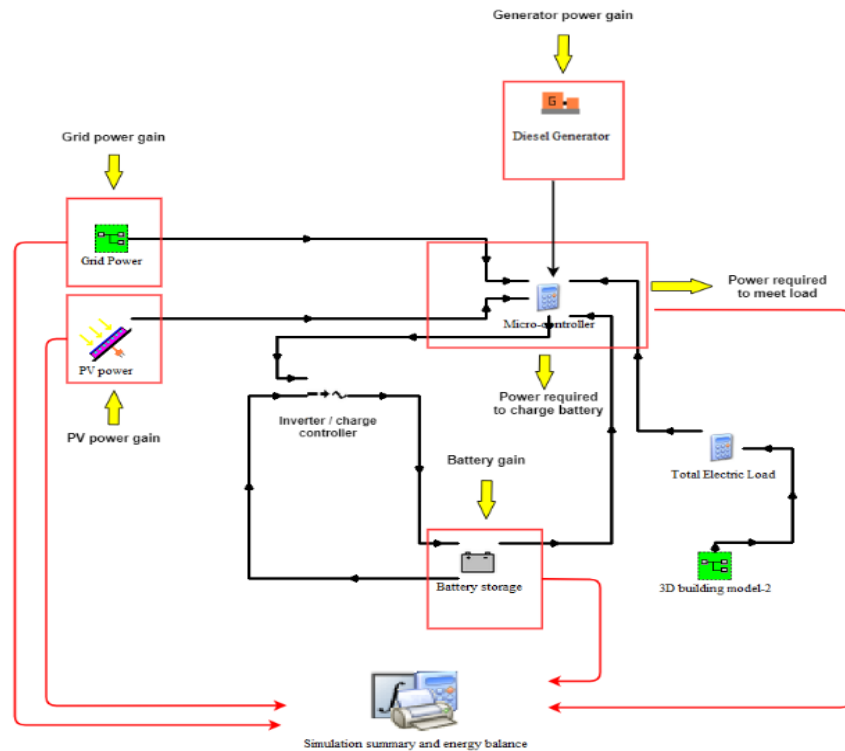
(a) System's power model energy balance
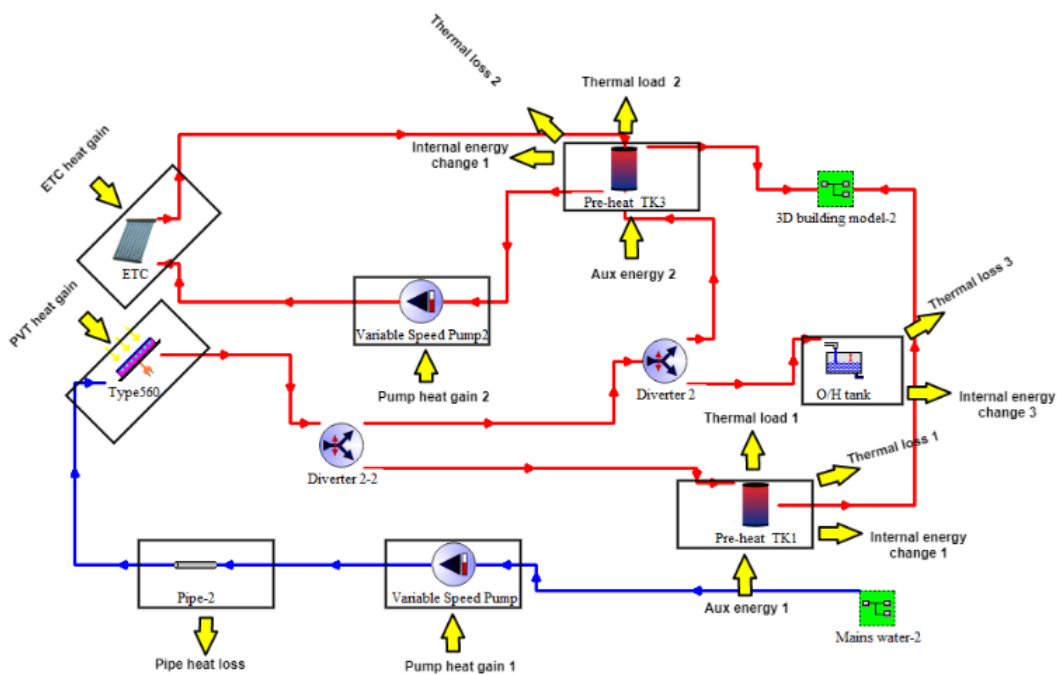
(b) System's thermal model energy balance

Figure 5. Schematic of power energy system balance (a) and the thermal energy balance (b).

2.5. Performance assessment

The energetic, economic, and environmental indices of energy systems are essential requirements to evaluate and compare the studied system with existing systems. Important indicators for the assessment and comparison include the collector efficiency, solar fraction, loss of power probability, and renewable fraction. The electrical efficiency η_{el} and thermal efficiency η_{th} are the electrical and thermal gains divided by the solar irradiance on the surface area of the solar collector as defined in (1). This indicator reveals the collector's capacity to convert the solar energy that falls on it to power and thermal energy. A lower value indicates that most solar energy is lost.

$$\eta_{total} = \eta_{el} + \eta_{th} = \frac{PV_{power} + Q_u}{I_T A_C} \qquad [38]\ (1)$$

where PV_{power} is the electrical power output of the PV module, and Q_u the useful thermal energy from the collector is. The Hottel–Whillier equation Hottel and Whillier equation defines Qu as the difference between thermal heat losses and the absorbed solar irradiance expressed as.

$$Q_u = A_c F_R (S - U_L(T_i - T_a)) \qquad [38]\ (2)$$

Another technical performance indicator is the Solar Fraction (SF). SF is the fraction of energy demand met from the solar system to the total demand expressed in (3). The SF value indicates ratio of the energy saving of the PVT in meeting the total energy demand of the building [39] [40], as defined in (3).

$$SF = \frac{\textbf{load met by RE energy sources}}{\textbf{Total energy demand}} \qquad [41]\ (3)$$

Technical matrices that measure system reliability indices are the Loss of Power Probability (LOLP). The LOLP is the probability that the energy system may not supply energy to meet demand at any given length of time. It is expressed as in (4).

$$LOLP = \int_0^t \left(\frac{\textbf{energy deficit}}{\textbf{energy demand}} \right) dt \qquad [42]\ (4)$$

To assess the mitigation impact of the energy system, the avoided carbon dioxide (ACO₂) emission displaced by the system is calculated based on the type of fuel substituted from (6). Therefore, the ACO₂ is calculated based using diesel generator as the reference system.

$$Avoided_{CO_2}\ Ratio = \frac{ACO_{2\,prop}}{CO_{2\,ref}} \qquad [43]\ (5)$$

$$ACO_2 = \textbf{fuel displaced} \times \textbf{Emission factor} \qquad [43]\ (6)$$

Recommended emission factors of $0.439 kgCO_2/kWh$ for grid power and $2.6kg\ CO_2/L$ for diesel generators in the case of Nigeria [43].

2.6. System economic assessment

The Net Present Value (NPV) of a project measures the project's profitability at any time of interest but is evaluated mainly at the end of the project life. This indicator shows the worth of the project based on the present value analysis method [44]. In simple terms, it is the worth of the project when all expenses have been deducted, as expressed in (7).

$$NPV = Cash_{inflow} - Cash_{outflow} \qquad [45]\ (7)$$

The $Cash_{inflow}$ is the total revenue obtained from the energy saved, while the $Cash_{outflow}$ is equal to the system TLCC.

The general rule is to "Accept" if NPV >0, "Reject" if NPV<0, and "Accept" if NPV = 0.

3. Results and Discussion

In this section, the findings of the study based on the method formulated in Section 2 are presented. The implications of the results are clearly explained.

3.1. System response to energy management and flow control strategies

The dynamic behavior of renewable energy systems is the system's response to the weather condition, energy management, and control strategy. This response provides the means of understanding the system characteristic under the different conditions as a check to the appropriateness of the system under the formulated energy management strategies. Figure 6 is the dynamic performance of the system based on an overcast sky (6th July to 7th July). As seen from figure 6, in part labeled A, the grid is only dispatched to meet just the load and charge the battery as the Fractional State of Charge (FSOC) of battery is seen to increase. Again, from the part labeled B, the power from the PV is not sufficient to meet electric demand and the battery is discharged to supplement for the short fall as indicated by the decline in the battery FSOC. A simple evaluation of the figure shows that grid power is only available for about 18 hours out of 48 hours. PV power and stored energy in the battery cover about 67% of total electric demand, and the battery is only discharged to a minimum of about 25% of its full capacity for only one hour even under extremely low average radiation as low as 250W/m². A relevant conclusion drawn from this result is that even on a day with an overcast sky level of radiation as low as 250W/m², with just 37.5% of grid power availability, the proposed model and control strategy is capable of meeting up to about 67% of the total electric load even above the minimum acceptable solar fraction of 30% as recommended by NREL for reasonable economic performance with a fast payback period [46], [47].

An annual assessment of the system solar fraction performance shows that the OPVETC hybrid system configuration meets more of the thermal load (87%) than the electrical load (73%) as shown in figure 7. An assessment of a similar solar photovoltaic thermal (PVT) system design by Hosouli *et al*. [48] to supply electrical and

thermal demand of a dairy farm in Germany revealed that the system meets only 9.7% and 51.9% of power and hot water demand respectively. Comparing the result in this study and the study of Hosouli *et al*. indicates that energy management and flow control strategy is critical in tailoring the performance of the system to the target objective. This finding is expected because most PVT collectors can only convert 9-21% of the solar energy incident on them to electrical power, with the remainder transformed to heat. As a result, using the same collector to supply both thermal and electrical loads yield a larger thermal solar fraction than an electrical solar fraction. Overall, the system has a solar percentage of 80%, indicating that the sun's energy is used to meet approximately 80% of the entire building demand (such as thermal and electrical). The implication of an 80% solar component is large environmental benefit of reducing emissions that increase system economic viability indicating the applicability of the established energy management to priotize renewable energy sources in the hybrid system.
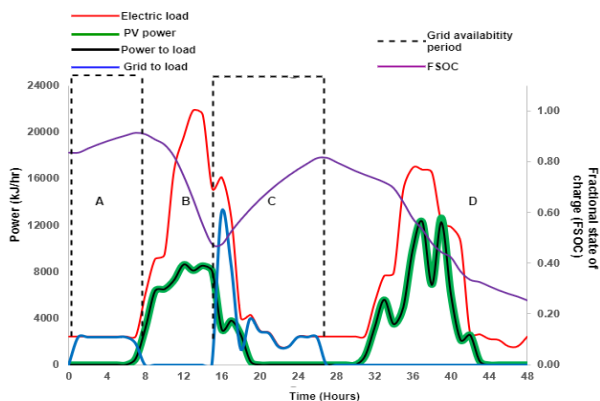

Figure 6. Dynamic performance of the system on an overcast day.
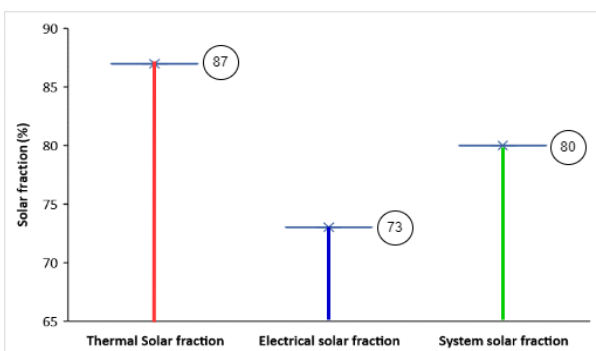

Figure 7. Annual solar fraction performance.

3.2. System reliability and environmental impact

The Loss of Load Probability (LOLP) is a suitable performance matrix to assess the system's

reliability. Table 2 is the monthly and annual evaluation of the loss of load probability for the OPVETC hybrid system architecture. It is seen from table 2 that in months with a high level of solar energy, the monthly average system reliability is higher than system reliability in months with a low level of solar energy. Overall, the OPVETC system architecture has an annual LOLP of 5.4%. An annual LOLP of 5.4% means that the system requires backup energy for 477 hours in a year (8760 hours) to be completely reliable. Consequently, for a diesel generator set used as a backup, as in this study, the generator-set is only operated for 477 hours per year with significant of reducing the operating cost and good environmental impact. Lower diesel operation and maintenance costs are financial benefits of the proposed configuration and energy management since its operated for just 477 hours (only 5% of the whole time in a year) and consumes a lower quantity of fuel and takes a long time before maintenance operation is carried out on the backup system with good savings in the energy cost of over 80%. This benefit can improve the profitability and sustainability of the hybrid energy system. Similarly, an Artificial Ecosystem-based Optimization (AEO) algorithm for the optimal sizing of a hybrid renewable energy conducted by [49] to satisfy the power need of consumers while maintaining reliability constraints shows savings in the cost of energy by about 40%.

Table 2. LOLP of the grid connected OPVETC system.

Month	Electric power demand (kWh/month)	Unmet electric power demand (kWh/month)	LOLP (%)
Jan	1364	5	0
Feb	1274	31	2
Mar	1546	39	3
Apr	1509	10	1
May	1584	176	11
Jun	1498	174	12
Jul	1492	94	6
Aug	1504	177	12
Sep	1437	139	10
Oct	1507	127	8
Nov	1381	0	0
Dec	1365	0	0
Annual Average	1455	80.9	5.4

The avoidable carbon dioxide ratio (ACO$_2$ Ratio) is a measure of the mitigative contribution of the renewable energy system to reducing the amount of CO$_2$ in the energy mix as a pathway for renewable energy technologies in the decarburization effort as required by the Paris Agreement (PA). Table 3 shows the avoided CO$_2$

emission evaluated using diesel fuel emission factor.

Table 3. Systems CO₂ emission and the computed ACO₂ Ratio.

| System configuration	ACO₂ (kg/yr)	ACO₂_ratio (%)
OPVETC	59137	78.8

As seen in table 3, the OPVETC hybrid energy system has an avoided CO_2/yr of 59,139kg/yr with an avoidable CO_2 ratio of about 78.8%. The roadmap to limit global warming to +1.5 °C requires that global emissions be cut down by about 7.6%/yr between 2020 and 2030 [50]. Therefore, the evaluated ACO_2 ratio of 78.8%/yr indicates that the proposed hybrid OPVETC operated based on the developed unreliable grid energy management to meet health center energy demand is an excellent option to cut the emission from the building sector. Again, since building energy consumption represents about 49% of Nigeria's total energy demand [51], the adoption of this technology in residential buildings could be a potential area for the country to target to keep to its CO_2 reduction target and make an effort to increase access to power in rural communities.

### 3.3. Model validation based on response to control logic

The formulated system model is validated and verified based on the expected dynamic performance of the entire system coordinated and controlled using the developed energy and flow control strategy. A careful observation of figure 8 shows that the dynamic behavior of the system meets all the mentioned requirements as formulated in the developed energy management and control strategy. From figure 8, the green line shows the power used to charge the battery storage. The battery is discharged only in periods when the grid and PV power are not available, as evident by the downward decrease of the battery fractional state of charge (FSOC) as shown in the graph. The power to the battery (green line) shows an exponential decrease when it is charged by the grid power. This behavior is in fulfilment of charging with only 10% of the battery capacity to ensure a longer period of discharge.

Further examination shows that the battery is only set to discharge to a maximum of 80% of its capacity in prolonged grid outages corresponding to a period with poor PV power generation due to cloudy and overcast sky conditions as expected as seen in figure 9. Remarkably, it is clear from point 'A' that the moment the power generated from the PV is more than the load, the excess is used to charge the battery if the FSOC of the battery is

less than 100%. This inspection is another technique that helps to fine-tune the developed energy model until the desired condition is met based on the reliability and economic objectives. Overall, the dispatch control strategy is successfully implemented. Therefore, the developed model for the simulation of the actual system, to a reasonable extent, mimics the expected behavior and control strategy.
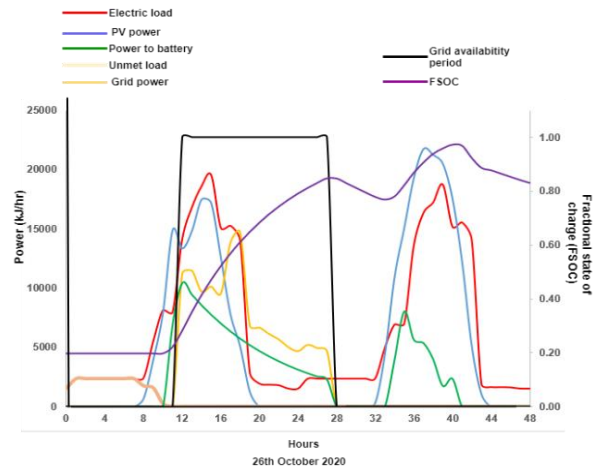
Figure 8. System behavior on typical days with grid availability and grid outage.
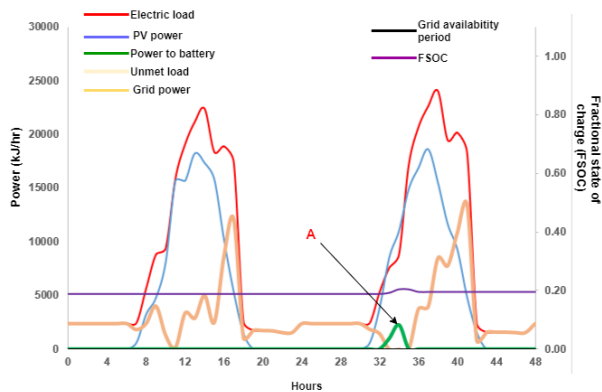
Figure 9. Dynamic behavior of the system on days with no grid power.

3.4. Energy balance analysis

For energy system modelling with the target of meeting a specific load, the model requirement is that the energy supply across all system boundaries should be balanced (not significantly in excess of the target load). Table 4 is the monthly and annual summary of the energy balance error obtained from the energy balance subroutine (Type 28) based on the electrical energy flows across the system boundary. From table 5, the difference between all electrical gains and losses across the system boundary is 1.28%. Comparing the model error of 1.28% for model power prediction based on the energy balance analysis and the model error of 1.48% of a study

conducted by [49] using the mean percentage error analysis, the model in this study has lower error. However, the two studies show error below the 2% tolerance benchmark implying that the model in this study is appropriately set up with not much excess electrical energy introduced into the system.

Similarly, table 5 shows an energy balance error of 1.49%, implying that the components are not oversized that leads to unnecessary increase in system cost but appropriately sized to meet the thermal load with not much excess thermal energy introduced into the system. On the other hand, it equally implies that the energy sources are not undersized to lead to system unreliability.

Table 4. Analysis of the formulated model power energy balance.

Months	Gains (kWh/month)				Losses (kWh/month)			Energy balance (%)
	Diesel power	PVT power	Grid power	Power to battery	Electrical Load	Battery power to load	Dumped energy	
Jan	4.6	1363.6	194.1	282.1	1364.2	227.1	115.7	1.54
Feb	31.1	1128.9	227.6	284.9	1273.9	270.0	76.2	1.38
Mar	38.9	1263.4	324.1	349.4	1546.5	347.2	52.4	1.29
Apr	10.1	1392.5	270.3	349.5	1508.7	296.6	83.5	1.43
May	176.3	1116.5	303.5	303.2	1584.2	314.5	0.9	1.18
Jun	173.5	975.9	392.1	330.8	1497.6	307.7	1.2	1.07
Jul	94.0	952.0	499.8	360.0	1492.3	355.9	30.0	1.02
Aug	177.1	922.9	446.5	335.1	1504.3	331.2	19.7	1.00
Sep	138.6	1078.3	333.0	348.0	1437.0	309.5	52.6	1.18
Oct	126.6	1169.5	318.8	314.4	1507.0	293.3	63.3	1.24
Nov	0.0	1457.3	130.5	311.2	1380.5	292.4	159.3	1.56
Dec	0.0	1345.5	204.7	291.4	1365.4	263.7	130.2	1.50
Sum	**970.8**	**14166.1**	**3645.1**	**3860.0**	**17461.6**	**3609.0**	**784.8**	**1.28**

Table 5. Analysis of the formulated model thermal energy balance.

Months	Gains (kWh/month)		Losses (kWh/month)				Energy balance (%)
	Collector thermal gain	Auxiliary heat	Thermal load	Tank loss	Pipe loss	Internal energy	
Jan	4645.35	63.74	4518.01	103.50	1.36	0.0081	1.85
Feb	3895.36	73.41	3817.31	92.32	1.26	0.0000	1.47
Mar	4487.57	87.56	4367.05	105.34	1.48	0.0008	2.24
Apr	4979.88	39.14	4759.34	113.47	1.49	0.0012	2.93
May	3597.17	121.45	3600.80	96.57	1.52	0.0009	0.53
Jun	2934.76	198.90	3035.48	83.07	1.44	0.0000	0.44
Jul	2691.36	253.32	2867.83	80.71	1.45	0.0005	0.18
Aug	2591.38	292.06	2809.87	76.73	1.42	0.0005	0.16
Sep	3359.81	193.29	3415.67	89.21	1.41	0.0005	1.33
Oct	3836.80	118.84	3827.20	95.49	1.48	0.0004	0.80
Nov	5119.98	32.98	4903.79	105.54	1.41	0.0005	2.80
Dec	4579.71	55.31	4450.56	103.80	1.37	0.0016	1.73
Summary	**46719.12**	**1530.01**	**46372.92**	**1145.76**	**17.09**	**0.0056**	**1.49**

3.5. System net present value (NPV)

The cumulative cash flow diagram is another way of examining the worth of the project at a specific period for the entire duration of the project lifetime. Figure 10 is the cumulative cash flow of the OPVETC system architecture during the 25 years lifetime of the project evaluated based on the economic indices shown in table 6 and table 7. As observed from Figure 10, the net present worth (NPV) is negative in the early part of the project lifetime before the payback period of 6.9 years. This implies that for investment in this energy system, the project profitability starts only after a minimum of 7 years. This indicates a lower risk compared to similar studies in Anthem with 15.6 years payback period, and 11.6 years payback

period in Zaragoza [52]. Notably, the NPV of the system declines relative to the previous year NPV any time the components are replaced as indicated in year 10, 15, and 20 on the cashflow diagram. Interestingly, the NPV is still positive even after the years the system components are replaced. This observation can be explained by the fact that the energy saving from the system is huge enough to offset the replacement cost. The result implies significant economic benefit as seen from the NPV of $36,985 at the end of the project lifetime making the business outlook and investment in this technology for domestic application an attractive venture.
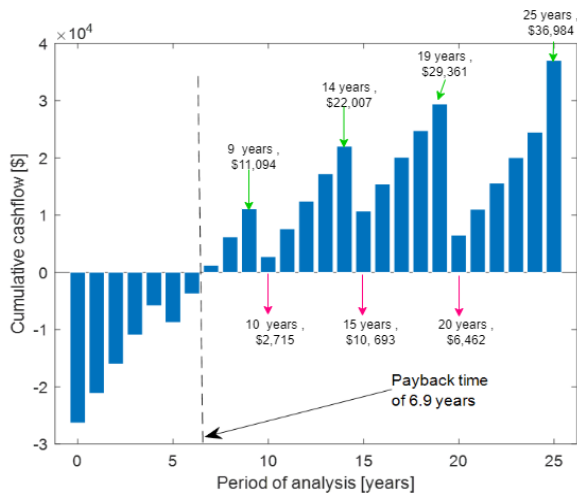
Figure 10. OPVETC cumulative cash flow during project lifetime.

Table 6. System components and the current market prices of system components.

SN	Parameter	Qty	Unit cost (USD)	Reference
1	PVT collectors (1.63 m²⁾	33	480	[53]
2	ETC (1.63 m²)	2	295	
3	Hot water tank (0.3 m³)	2	380	[54]
4	Controller	2	210	[54]
5	Battery (75 Amp, 24 volts)	15	380	
6`	Inverters (8 kW)	1	960	[24]
7	Gen set 20 kW	1	1580	[54]

Table 7. Parameters for system economic assessment.

SN	Economic index	Value	Unit	References
1	Inflation rate	14	%	[55]
2	Annual discount rate	6	%	[55]
3	Degradation factor	0.5	%	[54]
4	Cost of diesel fuel	0.48	$/L	[56]
5	Cost of grid power	0.10	$/kWh	[54]
6	Battery lifetime	5	years	[53]
7	Inverter lifetime	10	years	[53]
8`	Diesel gen lifetime	15000	hours	[53]

4. Conclusion

The TRNSYS 18 software was used to successfully create and evaluate a numerical model based on a novel open loop photo-voltaic evacuated tube collector coupled to grid power and characterized by random power loss. The system has good applications even in areas with poor solar resources, as shown by the results, which show that even on days with overcast skies and radiation levels as low as 250W/m² and only 37.5% of grid power availability, the proposed model has solar fraction of about 67% of the total electric load, which is higher than the minimum acceptable solar fraction of 30% as recommended by NREL for reasonable economic performance

with solar energy. The system's economic assessment further indicated a large economic profit of $36,985 as the net present value at the end of the project's lifetime, indicating that investing in this technology for domestic use is a profitable venture. Overall, the OPVETC system architecture operated based on the random grid power failure energy management has an annual Loss of Load Probability (LOLP) of 5.4%. As a result of low LOLP, the proposed system and energy management has improved profitability with significant environmental impact as the OPVETC hybrid energy system has an avoidable CO_2 ratio of about 78.8%. In order to keep global warming to +1.5°C, global emissions must be reduced by 7.6%/year between 2020 and 2030. Therefore, the proposed hybrid OPVETC operated based on the created unreliable grid energy management to fulfill health center energy demand is a great choice to reduce emissions from the building sector, as shown by the evaluated avoidable CO2 ratio of 78.8%/yr. Additionally, the payback duration of 6.9 years suggests a lower risk compared to comparable studies in Anthem with a payback period of 15.6 years and in Zaragoza with a payback period of 11.6 years.

5. Nomenclature

Abbreviations

ACO₂	Avoided Carbon Dioxide
BSOC	Battery State of Charge
DOD	Depth of discharge
EMS	Energy management Strategy
ETC	Evacuated Tube Collector
FEL	Follow-Electric-Load
FSOC	Fractional State of Charge
GA	Genetic Algorithm
GSHP	Ground Source Heat Pump
IFC	International Finance and Cooperation
NREL	National Renewable Energy Laboratory
NPV	Net Present Value
OPVETC	Open Loop Photovoltaic Evacuated Tube Collector
PV	Photovoltaic
PVT	Photovoltaic-Thermal
SCR	Self-consumption Ratio
SSR	Self-sufficient Ratio
SF	Solar fraction
SOC	State of Charge
TRNSYS	Transient System

Symbols

η_{el}	Electrical efficiency
η_{total}	Total efficiency
η_{th}	Thermal efficiency
A_C	Cross-sectional area
F_R	Heat removal factor

142

I_T	Radiation on tilted surfaces
$LOLP$	Loss of load probability
PV_{power}	Photovoltaic power
Q_u	Useful energy
S	Absorbed solar energy
T_i	Collector water inlet temperature
T_a	Ambient temperature
$TLCC$	Total Life Cycle Cost
U_L	Collector heat lost coefficient

6. Acknowledgements

7. References

[1] L. O. Aghenta and M. T. Iqbal, "Design and Dynamic Modelling of a Hybrid Power System for a House in Nigeria," *Int. J. Photoenergy*, Vol. 2019, pp. 1–13, 2019, doi: 10.1155/2019/6501785.

[2] A. S. Aziz, M. F. N. Tajuddin, M. R. Adzman, A. Azmi, and M. A. M. Ramli, "Optimization and sensitivity analysis of standalone hybrid energy systems for rural electrification: A case study of Iraq," *Renew. Energy*, Vol. 138, pp. 775–792, 2019, doi: 10.1016/j.renene.2019.02.004.

[3] A. Aly, M. Moner-Girona, S. Szabó, A. B. Pedersen, and S. S. Jensen, "Barriers to Large-scale Solar Power in Tanzania," *Energy Sustain. Dev.*, vol. 48, pp. 43–58, 2019, doi: 10.1016/j.esd.2018.10.009.

[4] M. Herrando, A. Ramos, J. Freeman, I. Zabalza, and C. N. Markides, "Technoeconomic modelling and optimisation of solar combined heat and power systems based on flat-box PVT collectors for domestic applications," *Energy Convers. Manag.*, Vol. 175, No. March, pp. 67–85, 2018, doi: 10.1016/j.enconman.2018.07.045.

[5] C. O. Okoye and B. C. Oranekwu-Okoye, "Economic feasibility of solar PV system for rural electrification in Sub-Sahara Africa," *Renew. Sustain. Energy Rev.*, Vol. 82, No. July 2016, pp. 2537–2547, 2018, doi: 10.1016/j.rser.2017.09.054.

[6] O. Rodriguez-Hernandez, M. Martinez, C. Lopez-Villalobos, H. Garcia, and R. Campos-Amezcua, "Techno-economic feasibility study of small wind turbines in the Valley of Mexico metropolitan area," *Energies*, Vol. 12, No. 5, pp. 1–26, 2019, doi: 10.3390/en12050890.

[7] A. Behzadi, E. Thorin, C. Duwig, and S. Sadrizadeh, "Supply-demand side management of a building energy system driven by solar and biomass in Stockholm: A smart integration with minimal cost and emission," *Energy Convers. Manag.*, vol. 292, no. July, p. 117420, 2023, doi: 10.1016/j.enconman.2023.117420.

[8] F. J. Vivas, A. De las Heras, F. Segura, and J. M. Andújar, "A review of energy management strategies for renewable hybrid energy systems with hydrogen backup," *Renew. Sustain. Energy Rev.*, Vol. 82, No. April 2016, pp. 126–155, 2018, doi: 10.1016/j.rser.2017.09.014.

[9] A. F. Crossland, O. H. Anuta, and N. S. Wade, "A socio-technical approach to increasing the battery lifetime of off-grid photovoltaic systems applied to a case study in Rwanda," *Renew. Energy*, Vol. 83, pp. 30–40, Nov. 2015, doi: 10.1016/J.RENENE.2015.04.020.

[10] P. García, J. P. Torreglosa, L. M. Fernández, and F. Jurado, "Optimal energy management system for stand-alone wind turbine/photovoltaic/hydrogen/battery hybrid system with supervisory control based on fuzzy logic," *Int. J. Hydrogen Energy*, vol. 38, no. 33, pp. 14146–14158, Nov. 2013, doi: 10.1016/J.IJHYDENE.2013.08.106.

[11] M. S. Behzadi and M. Niasati, "Comparative performance analysis of a hybrid PV/FC/battery stand-alone system using different power management strategies and sizing approaches," *Int. J. Hydrogen Energy*, Vol. 40, No. 1, pp. 538–548, Jan. 2015, doi: 10.1016/J.IJHYDENE.2014.10.097.

[12] G. Cau, D. Cocco, M. Petrollese, S. Knudsen Kær, and C. Milan, "Energy management strategy based on short-term generation scheduling for a renewable microgrid using a hydrogen storage system," *Energy Convers. Manag.*, Vol. 87, pp. 820–831, Nov. 2014, doi: 10.1016/J.ENCONMAN.2014.07.078.

[13] A. Merabet, A. Al-Durra, and E. F. El-Saadany, "Energy management system for optimal cost and storage utilization of renewable hybrid energy microgrid," *Energy Convers. Manag.*, Vol. 252, p. 115116, Jan. 2022, doi: 10.1016/J.ENCONMAN.2021.115116.

[14] R. Kaluthanthrige and A. D. Rajapakse, "Demand response integrated day-ahead energy management strategy for remote off-grid hybrid renewable energy systems," *Int. J. Electr. Power Energy Syst.*, Vol. 129, p. 106731, Jul. 2021, doi: 10.1016/J.IJEPES.2020.106731.

[15] S. Bhattacharjee and C. Nandi, "Design of a voting based smart energy management system of the renewable energy based hybrid energy system for a small community," *Energy*, Vol. 214, p. 118977, Jan. 2021, doi: 10.1016/J.ENERGY.2020.118977.

[16] M. Jafari and Z. Malekjamshidi, "Optimal energy management of a residential-based hybrid renewable energy system using rule-based real-time control and 2D dynamic programming optimization method," *Renew. Energy*, Vol. 146, pp. 254–266, Feb. 2020, doi: 10.1016/J.RENENE.2019.06.123.

[17] P. Rullo, L. Braccia, P. Luppi, D. Zumoffen, and D. Feroldi, "Integration of sizing and energy management based on economic predictive control for

standalone hybrid renewable energy systems," *Renew. Energy*, vol. 140, pp. 436–451, 2019, doi: 10.1016/j.renene.2019.03.074.

[18] A. Mohamed and O. Mohammed, "Real-time energy management scheme for hybrid renewable energy systems in smart grid applications," *Electr. Power Syst. Res.*, Vol. 96, pp. 133–143, Mar. 2013, doi: 10.1016/J.EPSR.2012.10.015.

[19] Q. Ma, X. Huang, F. Wang, C. Xu, R. Babaei, and H. Ahmadian, "Optimal sizing and feasibility analysis of grid-isolated renewable hybrid microgrids: Effects of energy management controllers," *Energy*, Vol. 240, p. 122503, Feb. 2022, doi: 10.1016/J.ENERGY.2021.122503.

[20] L. Xia, Z. Ma, G. Kokogiannakis, S. Wang, and X. Gong, "A model-based optimal control strategy for ground source heat pump systems with integrated solar photovoltaic thermal collectors," *Appl. Energy*, Vol. 228, pp. 1399–1412, Oct. 2018, doi: 10.1016/J.APENERGY.2018.07.026.

[21] W. Liu *et al.*, "Smart Micro-grid System with Wind/PV/Battery," *Energy Procedia*, Vol. 152, pp. 1212–1217, 2018, doi: 10.1016/j.egypro.2018.09.171.

[22] N. H. Saad, A. A. El-Sattar, and A. E. A. M. Mansour, "A novel control strategy for grid connected hybrid renewable energy systems using improved particle swarm optimization," *Ain Shams Eng. J.*, Vol. 9, No. 4, pp. 2195–2214, 2018, doi: 10.1016/j.asej.2017.03.009.

[23] A. Allouhi, "A novel grid-connected solar PV-thermal/wind integrated system for simultaneous electricity and heat generation in single family buildings," *J. Clean. Prod.*, Vol. 320, No. July, p. 128518, 2021, doi: 10.1016/j.jclepro.2021.128518.

[24] C. O. Anyaeche, T. Akappo, and A. O. Adeodu, "Optimisation of Hybrid Energy System Production Parameters for Electricity Power Generation in Nigeria," *Energy Power Eng.*, Vol. 10, pp. 198–211, 2018, doi: 10.4236/epe.2018.105014.

[25] International Finance Corporation, "Off-grid Solar Market Trends Report 2018," Washington, D.C., 2018. doi: 10.1017/CBO9781107415324.004.

[26] D. Jonas, M. Lämmle, D. Theis, S. Schneider, and G. Frey, "Performance modeling of PVT collectors: Implementation, validation and parameter identification approach using TRNSYS," *Sol. Energy*, Vol. 193, No. September, pp. 51–64, 2019, doi: 10.1016/j.solener.2019.09.047.

[27] A. Zarrella, G. Emmi, J. Vivian, L. Croci, and G. Besagni, "The validation of a novel lumped parameter model for photovoltaic thermal hybrid solar collectors: a new TRNSYS type," *Energy Convers. Manag.*, Vol. 188, No. March, pp. 414–428, 2019, doi: 10.1016/j.enconman.2019.03.030.

[28] M. B. Sanjareh, M. H. Nazari, G. B. Gharehpetian, R. Ahmadiahangar, and A. Rosin, "Optimal scheduling of HVACs in islanded residential microgrids to reduce BESS size considering effect of discharge duration on voltage and capacity of battery cells," *Sustain. Energy, Grids Networks*, Vol. 25, p. 100424, Mar. 2021, doi: 10.1016/J.SEGAN.2020.100424.

[29] D. Jie, J. Seuss, L. Suneja, and R. G. Harley, "SoC feedback control for wind and ess hybrid power system frequency regulation," *IEEE J. Emerg. Sel. Top. Power Electron.*, Vol. 2, No. 1, pp. 79–86, Mar. 2014, doi: 10.1109/JESTPE.2013.2289991.

[30] S. G. Sigarchian, "Small Scale Decentralized Energy Systems optimization and performance analysis," KTH School of Industrial Engineering and Management, 2018 [Online]. Available: http://www.diva-portal.org/smash/record.jsf?pid=diva2%3A1206702&dswid=-4627.

[31] W. Pang, B. C. Duck, C. J. Fell, G. J. Wilson, W. Zhao, and H. Yan, "Influence of multiple factors on performance of photovoltaic-thermal modules," *Sol. Energy*, Vol. 214, No. November 2020, pp. 642–654, 2021, doi: 10.1016/j.solener.2020.11.050.

[32] H. B. C. El Hocine, K. Touafek, F. Kerrour, H. Haloui, and A. Khelifa, "Model Validation of an Empirical Photovoltaic Thermal (PV/T) Collector," 2015. doi: 10.1016/j.egypro.2015.07.749.

[33] S. Bae and Y. Nam, "Comparison between experiment and simulation for the development of a Tri-generation system using photovoltaic-thermal and ground source heat pump," *Energy Build.*, Vol. 231, p. 110623, 2021, doi: 10.1016/j.enbuild.2020.110623.

[34] P. Eguía-Oller, S. Martínez-Mariño, E. Granada-Álvarez, and L. Febrero-Garrido, "Empirical validation of a multizone building model coupled with an air flow network under complex realistic situations," *Energy Build.*, Vol. 249, p. 111197, Oct. 2021, doi: 10.1016/J.ENBUILD.2021.111197.

[35] A. Rasheed, C. S. Kwak, H. T. Kim, and H. W. Lee, "Building energy an simulation model for analyzing energy saving options of multi-span greenhouses," *Appl. Sci.*, Vol. 10, No. 19, pp. 1–23, 2020, doi: 10.3390/app10196884.

[36] A. Mehmood, A. Waqas, Z. Said, S. M. A. Rahman, and M. Akram, "Performance evaluation of solar water heating system with heat pipe evacuated tubes provided with natural gas backup," *Energy Reports*, Vol. 5, pp. 1432–1444, Nov. 2019, doi: 10.1016/J.EGYR.2019.10.002.

[37] S. A. Klein *et al.*, *TRNSYS 18: A Transient System Simulation Program, Solar Energy Laboratory*. Madison, WI 53703 – U.S.A.: University of Wisconsin, 2017.

[38] A. N. Al-Shamani, K. Sopian, S. Mat, H. A. Hasan, A. M. Abed, and M. H. Ruslan, "Experimental studies of rectangular tube absorber photovoltaic

thermal collector with various types of nanofluids under the tropical climate conditions," *Energy Convers. Manag.*, Vol. 124, pp. 528–542, 2016, doi: 10.1016/j.enconman.2016.07.052.

[39] F. J. Diez, L. M. Navas-Gracia, A. Martínez-Rodríguez, A. Correa-Guimaraes, and L. Chico-Santamarta, "Modelling of a flat-plate solar collector using artificial neural networks for different working fluid (water) flow rates," *Sol. Energy*, Vol. 188, pp. 1320–1331, Aug. 2019, doi: 10.1016/j.solener.2019.07.022.

[40] Y. H. Li and W. C. Kao, "Performance analysis and economic assessment of solar thermal and heat pump combisystems for subtropical and tropical region," *Sol. Energy*, Vol. 153, pp. 301–316, 2017, doi: 10.1016/j.solener.2017.05.067.

[41] S. Hoseinzadeh and R. Azadi, "Simulation and optimization of a solar-assisted heating and cooling system for a house in Northern of Iran," *J. Renew. Sustain. Energy*, Vol. 9, No. 4, 2017, doi: 10.1063/1.5000288.

[42] H. A. Kazem, T. Khatib, and K. Sopian, "Sizing of a standalone photovoltaic/battery system at minimum cost for remote housing electrification in Sohar, Oman," *Energy Build.*, Vol. 61, pp. 108–115, 2013, doi: 10.1016/j.enbuild.2013.02.011.

[43] C. Sam-Amobi, O. V. Ekechukwu, and C. B. Chukwuali, "A preliminary assessment of the energy related carbon emissions associated with hotels in Enugu Metropolis Nigeria," *AFRREV STECH An Int. J. Sci. Technol.*, Vol. 8, No. 2, pp. 19–30, 2019, doi: 10.4314/stech.v8i2.2.

[44] C. Outline, *Life-Cycle Cost and Energy Productivity Analyses*. Elsevier Inc., 2018. doi: 10.1016/B978-0-12-849869-9/00005-3.

[45] J. Liu, S. Cao, X. Chen, H. Yang, and J. Peng, "Energy planning of renewable applications in high-rise residential buildings integrating battery and hydrogen vehicle storage," *Appl. Energy*, Vol. 281, No. June 2020, p. 116038, 2021, doi: 10.1016/j.apenergy.2020.116038.

[46] P. Bendt, *Appropriate sizing of solar water heating system*. Springfield, VA: Solar Energy Research Institute, 1980. [Online]. Available: https://www.nrel.gov/docs/legosti/old/320.pdf

[47] S. Liu, B. Hao, X. Chen, C. Yao, and W. Zhou, "Analysis on limitation of Using Solar Fraction Ratio as Solar Hot Water System Design and Evaluation Index," *Energy Procedia*, Vol. 70, pp. 353–360, 2015, doi: 10.1016/j.egypro.2015.02.134.

[48] S. Hosouli *et al.*, "Evaluation of a solar photovoltaic thermal (PVT) system in a dairy farm in Germany," *Sol. Energy Adv.*, Vol. 3, No. January, p. 100035, 2023, doi: 10.1016/j.seja.2023.100035.

[49] H. O. Omotoso, A. M. Al-Shaalan, H. M. H. Farh, and A. A. Al-Shamma'a, "Techno-Economic Evaluation of Hybrid Energy Systems using Artificial Ecosystem-based Optimization with Demand-side Management," *Electron.*, Vol. 11, No. 2, 2022, doi: 10.3390/electronics11020204.

[50] UNEP, "Emissions Gap Report 2019: Global progress report on climate action," 2019. [Online]. Available: https://www.unep.org/interactive/emissions-gap-report/2019/index.php

[51] J. Rouleau and L. Gosselin, "Impacts of the COVID-19 lockdown on energy consumption in a Canadian social housing building," *Appl. Energy*, Vol. 287, No. February, p. 116565, 2021, doi: 10.1016/j.apenergy.2021.116565.

[52] M. Herrando, A. Ramos, J. Freeman, I. Zabalza, and C. N. Markides, "Technoeconomic modelling and optimisation of solar combined heat and power systems based on flat-box PVT collectors for domestic applications," *Energy Convers. Manag.*, Vol. 175, pp. 67–85, Nov. 2018, doi: 10.1016/j.enconman.2018.07.045.

[53] M. Herrando, A. M. Pantaleo, K. Wang, and C. N. Markides, "Solar combined cooling, heating and power systems based on hybrid PVT, PV or solar-thermal collectors for building applications," *Renew. Energy*, Vol. 143, pp. 637–647, Dec. 2019, doi: 10.1016/j.renene.2019.05.004.

[54] Made-in-China, "Solar pump system controller," 2021. https://mcabattery.en.made-in-china.com/product/LvRmrfouRzYg/China-High-Quality-24V-110ah-Gel-Sealed-Lead-Acid-Battery.html (accessed Mar. 05, 2021).

[55] U. K. Elinwa, J. E. Ogbeba, and O. P. Agboola, "Cleaner energy in Nigeria residential housing," *Results Eng.*, Vol. 9, No. January 2020, p. 100103, 2021, doi: 10.1016/j.rineng.2020.100103.

[56] GlobalPetrolPrice.com, "Nigeria Diesel prices," *GlobalPetrolPrice.com*, 2021. https://www.globalpetrolprices.com/Nigeria/diesel_prices/ (accessed Mar. 04, 2021).